Title
A 8Be IDENTIFIER AND ITS APPLICATION TO THE (a,8Be) REACTION

Authors
Wozniak, G.J.
Jelley, N.A.
Cerny, Joseph.

Publication Date
1974-03-01

Submitted to Nuclear Instruments
and Methods

LBL-2374
Preprint c.2

A ^{8}Be IDENTIFIER AND ITS APPLICATION TO THE (α,^{8}Be) REACTION

G. J. Wozniak, N. A. Jelley and Joseph Cerny

March 1974

Prepared for the U. S. Atomic Energy Commission
under Contract W-7405-ENG-48

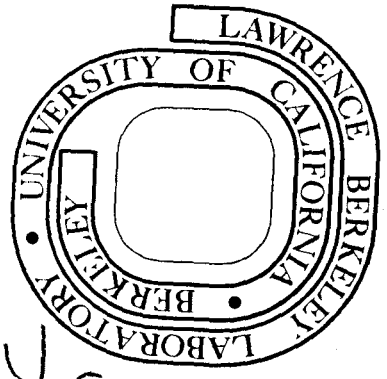

LBL-2374
c.2

DISCLAIMER

A ^{8}Be IDENTIFIER AND ITS APPLICATION TO THE (α,^{8}Be) REACTION*

G. J. Wozniak, N. A. Jelley, and Joseph Cerny

Department of Chemistry and
Lawrence Berkeley Laboratory
University of California
Berkeley, California 94720

March 1974

Abstract:

A ^{8}Be identifier consisting of a divided collimator, a transmission (ΔE) detector and a position-sensitive E detector has been designed. A solid angle of $\sim$ 6 msr is subtended, providing efficient detection of 35 - 70 MeV ^{8}Be events. Both a simple identifier, employing a single ΔE detector, and a modified identifier, using twin transmission detectors with subnanosecond pileup rejection, are described in detail. On light targets ($A \leq 16$), 400 keV ^{8}Be energy resolution was obtained at a high counting rate (50 K cps). The smallest absolute cross sections observable were, at 20 K cps, 1 μb/sr (simple identifier) and, at 50 K cps, 0.1 μb/sr (modified identifier). Results from solid and gas targets are discussed.

*Work performed under the auspices of the U. S. Atomic Energy Commission.

A ^{8}Be IDENTIFIER AND ITS APPLICATION TO THE (α, ^{8}Be)

Contents

1. Introduction

The study of reactions with ^{8}Be nuclei as the detected particles is complicated by the fact that the ^{8}Be ground state decays promptly ($t_{1/2} \sim 10^{-16}$ sec), and therefore must be observed indirectly by means of its breakup α-particles. The essential difficulty lies in detecting these two α-particles with high efficiency, while at the same time accurately determining the energy and direction of the original ^{8}Be event.

Previous methods of detecting ^{8}Be nuclei fall into two general categories: those observing the two α-particles in coincidence in two separate detectors[1]), and those using a single counter telescope[2]). The latter technique utilizes the fact that two approximately equal-energy α-particles simultaneously traversing a ΔE-E telescope identify as a ^{7}Li event; however, the range of excitation that can typically be observed with this technique is limited[2]) to ∿10 MeV. Both of these methods rely on collimation to reduce kinematic broadening, so that one must strike a balance between detection efficiency and energy resolution, particularly on light targets. High efficiency requires a ^{8}Be identifier subtending a large solid angle, while a restricted solid angle is necessary for small kinematic broadening.

In the detection technique discussed below a position-sensitive detector is used to measure both the direction and the energy of a ^{8}Be event, thereby permitting both good detection efficiency and reasonable energy resolution. Although ^{8}Be events can then be selectively observed by employing a divided collimator before this detector (as shown below), substantial background reduction of chance coincident events can be achieved by also employing a transmission (ΔE) detector.

The ^{8}Be identifier--consisting of a divided collimator, a transmission detector and a position-sensitive E detector--was developed to study the α-transfer reaction (α, ^{8}Be) on p-shell targets[3]). Because of the large α-structure amplitude of ^{8}Be, this reaction is a very useful spectroscopic probe with which to investigate theoretical α-structure amplitudes, such as those given by Kurath[4]) for p-shell nuclei. Both a simple ^{8}Be identifier, employing a single ΔE detector, and a modified one, utilizing twin ΔE detectors with subnanosecond pileup rejection to achieve low backgrounds at high counting rates (50 K cps), are discussed.

2. ^{8}Be Decay

The decay of ^{8}Be ($^{8}\text{Be} \equiv {}^{8}\text{Be}_{gs}$, hereafter) is characterized by a single decay channel, a small breakup energy (Q = 0.092 MeV), two identical charged products (α-particles) and, since all the spins involved are zero, an isotropic distribution of the decay products in the center of mass. By designing a detection system optimized for high energy ^{8}Be events ($E_8 > 35$ MeV, $E_8 \equiv E_{^{8}\text{Be}}$) to which discussion below is restricted, advantage can be taken of the strong kinematic focussing of the α-particles into a narrow cone whose axis is in the direction of the original ^{8}Be nucleus, and whose half angle (β_{max}) is given by:

$$\beta_{max} = \arcsin\left[(Q/E_8)^{1/2}\right] \qquad \text{(see fig. 1)} \quad .$$

For high energy ^{8}Be events, β_{max} is small (< 2.9°) and the angles β_1 and β_2 are approximately equal [$|\beta_1-\beta_2|/\beta_{max} < 5.2\%$]. In this approximation, the radial distribution, R(r), of α-particles across a detector is given by:

$$R(r)dr = (r/r_m^2)(1 - r^2/r_m^2)^{-1/2}\, dr \quad ,$$

where $r_m = D \tan \beta_{max}$ (see fig. 1).

By integrating this expression over r, the fraction, F(r), of breakup α-particles which fall between r and r_m is given by:

$$F(r) = (1 - r^2/r_m^2)^{1/2} \quad .$$

From this it follows that 71% of the α-particles lie between $r = 0.7\ r_m$ and $r = r_m$. (This result can be visualized by realizing that 71% of the breakup α-particles have a direction in the center of mass corresponding to $\gamma \geq 45°$, which in the laboratory is equivalent to $r \geq 0.7\ r_m$ since $r = r_m \sin\gamma$, see fig. 1.)

3. Simple Identifier

3.1. POSITION-SENSITIVE DETECTOR

The distribution of the breakup α-particles suggests that, in order to detect a substantial fraction of the ^{8}Be events, a detector must subtend an angle at least as large as that of the breakup cone ($\sim 5°$). However, such a large angular acceptance allows considerable variation in the detection angle (θ_{lab}) of the ^{8}Be events. On light targets ($A \leq 16$), a typical value of $dE/d\theta$ is around 500 keV/deg for the $(\alpha, ^8Be)$ reaction at $E_\alpha \sim 65$ MeV. The substantial kinematic broadening that would arise from this large value of $dE/d\theta$ is avoided by using a position-sensitive detector (PSD). A particle striking such a detector generates both an energy signal (E), and a signal (XE) proportional to the product of the energy (E) and the distance of impact from one side of the detector (X) (see fig. 2a). For high energy ^{8}Be events, the breakup Q-value is small compared to the ^{8}Be energy, and so the two breakup α-particles have, to a first approximation, equal energies [$|E_1-E_2|/(E_1+E_2) < 10\%$]. On striking a position-sensitive detector, one α-particle therefore produces a signal $X_1E/2$, the other $X_2E/2$. Since both alphas arrive within a fraction of a nanosecond, the individual E and XE signals are automatically summed and the resultant E signal gives the energy of the ^{8}Be event. The position signal (X) obtained by dividing out the energy dependence is given by:

$$X = (X_1E/2 + X_2E/2)/(E/2 + E/2) = (X_1 + X_2)/2 \quad .$$

As can be seen from fig. 2a, this average position establishes the direction of the ^{8}Be event (θ_{lab}), and substantial kinematic broadening can therefore be avoided by gating the energy signals with position signals corresponding to a small angular range.

It is implied in the above derivation that the expression for X holds only to the extent that $E_1 = E_2$ and $\beta_1 = \beta_2$, and therefore that the direction of the ^{8}Be event (θ_{lab}) is correspondingly uncertain. In fact, θ_{lab} is more accurately determined since the differences in β and E closely cancel. Qualitatively, the α-particle with the lower energy has the larger β and hence the larger r, and vice versa (see fig. 1). Referring to figs. 1 and 2a, the direction of the ^{8}Be event is given by X, while XE/E division yields X', where:

$$X'-X = (1/2)\left(\frac{DQ}{E_8}\right)\sin 2\gamma \quad .$$

As mentioned above, a transmission (ΔE) detector is introduced to reduce background and this modifies the above expression to:

$$X'-X = (1/2)\left(\frac{DQ}{E_8-\Delta E}\right)\left(1+\frac{3\Delta E}{E_8}\right)\sin 2\gamma \quad .$$

This corresponds to an error in the angle θ_{lab} of $< 0.1^\circ$ for high energy ^{8}Be events[5]) detected with a counter telescope employing a 100 μm ΔE detector.

3.2. DIVIDED COLLIMATOR

While good efficiency and energy resolution can be obtained with a position-sensitive detector alone, numerous particle-stable nuclei would also be detected, and so obscure ^{8}Be events except when these happened to be more energetic. To avoid this limitation, the high probability that the angular separation of the two breakup α-particles is close to its maximum value ($\sim 5^\circ$) is exploited to selectively detect ^{8}Be events. This selectivity is accomplished by using a divided collimator, which has a post subtending $\sim 2^\circ$, to block out the central region of the position-sensitive detector, as is shown in fig. 2b.

Employing such a divided collimator eliminates particle-stable nuclei that are emitted within $\sim \pm 1^{\circ}$ of the center of the detector. However, a substantial fraction of the two α-particles from ^{8}Be nuclei emitted in this direction pass one on either side of the post. As indicated in fig. 2b, these events yield signals corresponding to the region of the position-sensitive detector masked by the post. Therefore, gating the energy signals by such position signals selects ^{8}Be events, while eliminating particle-stable nuclei.

3.3. TRANSMISSION DETECTOR

While a divided collimator and a position-sensitive detector would make a selective and efficient ^{8}Be detector, substantial background would arise at moderate counting rates ($\sim$ 15 K cps)[6] from chance-coincident particles arriving within the pulse pair resolving time of the detector. Nearly all of these intra-beam-burst pileup events are from particles which have sufficient energy to traverse the depleted depth of the PSD. Most of them, though, cannot be eliminated by using a reject detector, because commercially available PSDs have such thick undepleted back layers that a large fraction of these particles would fail to traverse the PSD. However, many background events can be eliminated by adding a transmission detector (see fig. 2b) and performing particle identification (PI) with the ΔE and E signals. For events stopping in the depleted depth of the PSD, an α-particle generates a PI signal given by:

$$PI(\alpha) = (E_{\alpha} + \Delta E_{\alpha})^{1.73} - E_{\alpha}^{1.73} \quad ,$$

while a ^{8}Be event generates the following signal:

$$PI(^8Be) = \left(E_{\alpha_1} + E_{\alpha_2} + \Delta E_{\alpha_1} + \Delta E_{\alpha_2}\right)^{1.73} - \left(E_{\alpha_1} + E_{\alpha_2}\right)^{1.73} \quad .$$

Since $E_{\alpha_1} \simeq E_{\alpha_2}$ and hence $\Delta E_{\alpha_1} \simeq \Delta E_{\alpha_2}$, this expression is closely approximated by:

$$PI(^8Be) = 2^{1.73}\ PI(\alpha) \quad .$$

Thus the α-particles from a ^{8}Be event identify as a peak in the PI output. However, pileup events from α-particles that traverse the depleted depth of the PSD give rise to PI signals falling substantially lower in the PI spectrum than $PI(^8Be)$, and so substantial background reduction is possible, at moderate counting rates, by setting a gate around the ^{8}Be PI peak.

3.4. DETECTION EFFICIENCY

When using the simple identifier, the magnitude of the acceptance solid angle (Ω_{acc}) for detecting ^{8}Be events is restricted to the solid angle subtended by the post of the divided collimator. Only a certain fraction of the ^{8}Be events emitted into Ω_{acc} are detected. This fraction is defined to be the detection efficiency (ε), and the product of ε and Ω_{acc} yields the effective solid angle ($\Omega_{eff} = \varepsilon \cdot \Omega_{acc}$) for detecting ^{8}Be events.

By increasing the vertical size of the post of the divided collimator, both the acceptance solid angle and the efficiency are increased. A larger ε results because ε is the average efficiency over the entire extent of the acceptance solid angle. This solid angle is necessarily small for a narrow post width (P) while the efficiency is zero for a post width greater than the diameter of the breakup cone ($d_m = 2\ r_m$). Thus there is an optimum post width corresponding

to the largest effective solid angle. This is illustrated in fig. 3(a) for the case of a circular divided collimator of diameter $\mathcal{D}$. When the collimator diameter is greater than that of the breakup cone, the optimum post width of $\sim 0.35\ d_m$ is essentially independent of $\mathcal{D}$. The ordinate scale depends on the energy of the ^{8}Be event that is being considered, since the apex angle of the breakup cone varies as $1/(E_8)^{1/2}$ for high energy events (see section 2).

In part b of fig. 3 is shown the dependence of the detection efficiency (ε) on the diameter of the collimator, for a post width of $0.4\ d_m$. . As $\mathcal{D}$ increases, ε also becomes larger. However, if the maximum counting rate in the identifier is limited by the electronics, the highest data acquisition rate is obtained not for the largest ε but when the ratio of the effective solid angle for the detection of ^{8}Be events compared to that for particle stable nuclei is greatest. This latter solid angle is that subtended by the open area of the divided collimator (Ω_{coll}). The ratio, $\Omega_{eff}/\Omega_{coll}$, is called the relative efficiency (ε_{rel}). Because of the finite extent of the breakup cone, there is an optimum diameter of the divided collimator for maximum relative efficiency. As can be seen from fig. 3(b) this maximum is obtained for $\mathcal{D} \sim 1.5\ d_m$. Over a restricted range of kinetic energies (35-70 MeV), the size of the breakup cone varies by only a small amount ($d_m \propto 1/(E_8)^{1/2}$), thus a fairly energy-independent and large ε_{rel} can be achieved. A rectangular divided collimator can also be used and similar considerations apply as for a circular one.

3.5. ELECTRONICS

A block diagram of the electronics for the simple ^{8}Be identifier is shown in fig. 4. Signals from the ΔE and E(PSD) feed three amplifier systems and a pileup rejector (PUR). This last unit establishes a coincidence (2τ = 50 ns) between the ΔE and E signals and inspects for pileup arising from different beam bursts over 1.5 microseconds. In the absence of such inter-beam-burst pileup a valid-event signal is generated.

To minimize deadtime caused by the high counting rate in the ΔE detector, double-delay line shaping is used to provide short signal shaping times and fast baseline recovery. Because signals from the E(PSD) have a slow and position dependent risetime, a linear amplifier with a two microsecond peaking time is used for both the E and XE signals. A pulse from the E amplifier is used to feed a pileup rejector which inspects over the duration ($\sim$ 8 μs) of the E signal (the counting rate in the E(PSD) is typically a factor of four less than in the ΔE). The E and XE signals are connected to a divider, which converts the position information into a time difference, and a time-to-amplitude converter is used to give a voltage signal proportional to the position. The ΔE and E signals feed a particle identifier. Both particle identification (PI) and position gates are set with single channel analyzers (SCAs) and energy spectra, gated by these, are collected on a Nuclear Data 4096 channel analyzer. Gated and ungated PI and position spectra are monitored during experiments.

4. Experimental Results (Simple Identifier)

In an initial study[3]) of the (α,^{8}Be) reaction on light targets, a simple identifier with a 125 μm ΔE detector (10 mm in diameter) and a 300 μm E(PSD) detector (10×50 mm) was used[7]). A circular divided collimator, with an acceptance angle of six degrees and a central post of two degrees, was placed seven and a half centimeters from the target. With this geometry, forward angle observations were possible to a minimum angle of twelve degrees, and near maximum relative efficiency (ε_{rel}) was attained for the range of ^{8}Be events stopped by the identifier (35-60 MeV). The beam spot size was equivalent to one degree and a one degree position gate was set. These conditions gave adequate energy resolution and detection efficiencies (ε) of 15-26% for 35-65 MeV ^{8}Be events emitted into the acceptance solid angle defined by the position gate. The intrinsic position resolution of the above detector was 1/2° and the two degree post width ensured the complete elimination of particle-stable nuclei from the central region of the position-sensitive detector.

The elimination of particle-stable nuclei is illustrated in the appropriate position spectrum shown in fig. 5(a). The upper spectrum was taken with an open circular collimator, and the lower with a circular divided one. The counts in the central region of the latter are from ^{8}Be events with a small number from intra-beam-burst pileup events. These spectra were collected at $\theta_{lab} = 15\pm3°$ during the bombardment of a carbon target with 65 MeV α-particles. The counting rate in the ΔE detector was 15 K cps. Only events satisfying an inter-beam-burst pileup condition, a ΔE energy SCA (set to eliminate Z=1 and 2 events) and an E-lower threshold of 8 MeV were recorded.

In fig. 5(b), PI spectra are shown of the events satisfying the one degree position gate indicated in part (a). The upper spectrum shows the identification of the particle-stable nuclei, ^{6}Li and ^{7}Li, with the relatively abundant ^{8}Be

events appearing as a shoulder on the ^{7}Li peak. The lower spectrum, collected with the divided collimator, is characterized by the absence of lithium isotopes and the occurrence of a single peak at the location predicted for ^{8}Be events by range-energy calculations[2]). Nearly all background events seen above and below this peak correspond to intra-beam-burst α-α pileup. A relatively small fraction of these correspond to both chance coincident α-particles stopping in the sensitive region of the PSD. The PI signals for these events lie close to the position of the ^{8}Be peak (∿ equal-energy α-particles). However, as the energy of one or both of the α-particles increases above the maximum capable of being stopped in the depleted region of the PSD, the PI signal rapidly decreases in magnitude[8]). Consequently, at moderate counting rates (15 K cps), nearly all pileup events are eliminated by setting a PI gate around the ^{8}Be peak.

An energy spectrum, taken in one hour with the simple identifier, of the ^{11}B(α,^{8}Be)^{7}Li reaction at θ_{lab} = 20° and E_{α} = 65 MeV is shown in fig. 6. A 100 μgm/cm^{2} ^{11}B target (enriched to 98%) was used and an experimental resolution of 600 keV was obtained at a counting rate in the ΔE detector of 19 K cps, which caused a 9% deadtime. Transitions populating the ground and second excited states[9]) of ^{7}Li are seen. Preferential population of these states is expected on the basis of calculated α-particle structure factors[4]). The measured cross-section to the ^{7}Li$_{gs}$ is 3.2 μb/sr at this angle, which, after allowing for the detection efficiency (23%), corresponds to an absolute cross-section of 14 μb/sr. Other spectra from the (α,^{8}Be) reaction on p-shell targets, taken with the simple identifier,

are presented in ref. [3]). No contribution from the (α, $^{8}Be^{*}$(2.9 MeV)) reaction[10]) was observed, which is in agreement with the low calculated detection efficiency ($\sim$ 0.5%) for $^{8}Be^{*}$ events. The moderately low level of counts above the $^{7}Li_{gs}$ peak is due to intra-beam-burst chance coincident events that fall within the ^{8}Be PI gate. This level of background is indicative of the background contribution to spectra taken at 19 K cps with the simple identifier, and is equivalent to an absolute differential cross section limit of $\sim$1 μb/sr.

5. Modified Identifier

5.1. TWIN TRANSMISSION DETECTORS

A substantial improvement to the simple identifier can be made by using, instead of a single ΔE, two ΔE detectors diffused side by side on a single silicon wafer (see fig. 7). An order-of-magnitude reduction of intra-beam-burst pileup can then be achieved by making a subnanosecond coincidence between these detectors. Further reduction in background is possible through a comparison of the energy loss in each detector.

Two 5.5×12 mm transmission detectors, ΔE_L and ΔE_R, separated by a one millimeter undiffused region were made on a 110 μm thick wafer. These twin detectors act as a large area detector when the left and right signals are added. Since the same wafer is used for both ΔE_L and ΔE_R, good uniformity, and hence good particle identification, is ensured. This technique takes advantage of the fact that the central region of the ΔE detector is not used since it is masked by the central post of the divided collimator.

Since in this approach a ^{8}Be event can be characterized by a fast coincidence between the ΔE detectors, rather than by a position signal corresponding to the masked region of the E(PSD), the post need only be wide enough to cover the dead region between the detectors. (In the limit of a post width of zero, the acceptance solid angle (Ω_{acc}) would be restricted to the solid angle subtended by the half width of the "divided" collimator.) The detection efficiency and the relative efficiency depend on the dimensions of the divided collimator in a similar way to that discussed in section 3, except that the acceptance solid angle is not restricted to the post width. As for the simple identifier, Ω_{acc} is defined by the setting of the position gate.

5.2. INTRA-BEAM-BURST PILEUP REJECTION

When ^{8}Be decays, the two breakup α-particles generally have different energies, and so different arrival times at the twin ΔE detectors. The maximum time difference (Δt_{max}) is given by:

$$\Delta t_{max} = 1.24\ D/E_8 \text{ nsec} ,$$

where D is the distance from the target to the ΔE detector, and E_8 is the energy of the ^{8}Be event. For $E_8 > 35$ MeV and D = 11.8 cm, Δt_{max} is less than 0.42 nanoseconds. Therefore by performing a subnanosecond coincidence, the background can be reduced by a factor of ten, since the typical beam burst width at the Berkeley 88-inch cyclotron is approximately five nanoseconds (at a frequency of 10 MHz).

To achieve subnanosecond timing, two fast preamplifiers are used, whose first stages are mounted on the holder for the twin ΔE detectors. These preamplifiers are similar to the one described in ref. [11]), but with a charge-sensitive (slow) output added to give greater energy stability. The FET in the first stage of the preamplifier is connected by a low inductance strip to the surface of the detector. This detector is made with a low sheet resistance (< 10 Ω/cm^2) and the short direct coupling produces very fast risetime pulses (< 2 ns).

The 110 μm twin transmission detectors have a low capacitance (∿ 70 pF), which gives a good signal to noise ratio, and they hold a high voltage gradient (2 volts/μm), which ensured fast (< 1 ns) collection of the deposited charge. As indicated in the block diagram of the electronics for the modified identifier (see fig. 8), the fast outputs of the ΔE_L and ΔE_R

preamplifiers feed two constant-fraction discriminators (CFD), which are connected to a time-to-amplitude converter (TAC). The range of α-particle energy deposited in the ΔE detectors varied between 4 and 11 MeV, but no time-walk-with-amplitude compensation is required for good time resolution, since ^{8}Be events generate ΔE_L and ΔE_R signals of approximately equal amplitude. By injecting charge on the detector surface with a fast pulser (< 1 ns risetime), a simulated ^{8}Be event ($\Delta E_L = \Delta E_R = 8.75$ MeV, $E_8 = 32$ MeV) gave a time resolution of 140 picoseconds FWHM.

5.3. RATIO REQUIREMENT

Since both breakup α-particles from a ^{8}Be event have similar energies, the energy loss of α_1 in ΔE_L is approximately equal to that of α_2 in ΔE_R. By calculating the ratio $R = \Delta E_L/(\Delta E_L + \Delta E_R)$, ^{8}Be events can be characterized by a ratio signal close to 1/2. Because two chance coincident particles will generally have different energies, setting an SCA about the ^{8}Be ratio peak will eliminate some intra-beam-burst pileup events. The division of the ΔE_L amplitude by the summed ΔE_L and ΔE_R amplitudes to yield the ratio R is carried out in a similar manner as the XE/E division (see fig. 8).

6. Experimental Results (Modified Identifier)

6.1. BACKGROUND REDUCTION

Figure 9 presents a TAC spectrum (ΔE_L(start) - ΔE_R(stop)) of events originating from the same beam burst. These events, from the bombardment of a ^{10}B target with 72.5 MeV α-particles, were detected with the modified identifier at $\theta_{lab} = 24^\circ$. The symmetric double peak is due to ^8Be events. Background counts are caused by fragmentation reactions and random chance coincident events associated with the high counting rate of 25 K cps in each of the ΔE detectors (intra-beam-burst rate ∿ 500 K cps). The full width at the base of the TAC peak (∿ 1 ns) reflects the minimum energy (∿ 30 MeV) ^8Be event that could be detected, and the central dip is the effect of collimation on the breakup α-particle velocity distribution. If the identifier had 100% detection efficiency and perfect time resolution, then the TAC peak would be rectangular with a width of 2 Δt_{max}. This is most closely realized for ^8Be nuclei emitted toward the center of the identifier. However, for those emitted off center, the first part of the breakup cone that is lost through collimation is the edge. Therefore, most of the ^8Be events emitted into the acceptance solid angle, that are not detected, correspond to the breakup α-particles having approximately equal velocities, and therefore equal time-of-flights, hence the central dip in the TAC spectrum.

In the spectrum shown in fig. 9, only events depositing more than 10 MeV in the E detector, and satisfying a ΔE_L - ΔE_R inter-beam-burst coincidence (2τ = 50 ns) and ΔE energy SCAs (set to eliminate Z = 1 and 3 particles), were recorded. The total number of intra-beam-burst background counts, expressed as a percentage of the number of ^8Be events, is 120% for the above conditions

(see (a) in fig. 9). As further SCA requirements are made: (b), (c), (d), and (e), the background decreases considerably with only a 25% loss in the number of ^{8}Be events which is almost entirely due to the setting of a restricted X gate ($X \equiv X_L + X_C + X_R$, see fig. 10(b)). The lowest background is achieved when the position signal is restricted to fall within the ^{8}Be acceptance angle (X SCA); the PI falls in the calculated region for ^{8}Be events (PI SCA); the ratio is close to one-half (R SCA); and the TAC signal corresponds to a time difference $\leq \Delta t_{max}$ (TAC SCA). All these conditions are characteristic of ^{8}Be events. With these requirements the total background in a ^{8}Be energy spectrum is 1% of the number of ^{8}Be events, at a counting rate of 25 K cps in each ΔE detector.

Figure 10 shows a particle identification and a position spectrum obtained with the SCA conditions discussed above, except that their respective SCAs were not required. In fig. 10(a) the PI spectrum is dominated by a single peak occuring in the expected location for ^{8}Be events[2]) with very little background above and below this peak. (The $\Delta E_L - \Delta E_R$ coincidence requirement eliminates particle stable nuclei.) The peaking of the position spectrum, shown in fig. 10(b), at 24° (the angle of the center line of the divided collimator's post) arises because ^{8}Be nuclei emitted in this direction have the largest probability of yielding breakup α-particles which satisfy the $\Delta E_L - \Delta E_R$ coincidence condition.

A ratio spectrum, with the above PI and X SCA requirements, is given in fig. 11(b). The double peaking in this spectrum corresponds to that seen in the TAC spectrum shown in fig. 9. If the lower velocity alpha from a ^{8}Be event traverses ΔE_L and the higher velocity one traverses ΔE_R, this corresponds to a negative time difference in the TAC spectrum. It also corresponds to a higher ΔE_L energy loss ($dE/dx \propto MZ^2/E$), and therefore a ratio greater than one-half. This equivalence is demonstrated in fig. 11(c) (ii).

In fig. 11(c) (i) a TAC spectrum, routed by the wider R SCA, is shown. The shape of this peak is closely predicted as can be seen from the calculated[5]) peak shapes for 45 and 65 MeV ^{8}Be events given in part (a). (The asymmetry in the experimentally observed TAC peak of fig. 11(c) (i), is due to a slight asymmetry in the position gates.)

The relationship between the amplitude of the ratio (R) and that of the TAC (T), illustrated in fig. 11(c) (ii), demonstrates that a factor of 3 to 4 further background reduction is possible. Expressing $R = R_o + \Delta R$ and $T = T_o + \Delta T$, where R_o and T_o correspond to a ratio of one-half and to a time difference of zero, respectively, yields:

$$\Delta R \propto \Delta T \cdot (E_8)^{1/2} \quad .$$

This relationship could be calculated using a computer. Alternatively, a good analogue approximation would be to set an SCA about the sum of R and T, since the variation in $(E_8)^{1/2}$ is small for 35-70 MeV ^{8}Be events.

6.2. ENERGY SPECTRA

In the modified identifier, besides requiring a fast coincidence and comparing the relative energy loss in the twin transmission detectors, larger area detectors were used. These allowed the identifier to be placed farther from the target while subtending the same solid angle as before, and hence maintaining good detection efficiency. At this greater distance (D = 11.8 cm), more forward angles could be studied and the contribution of the beam spot size to the energy resolution was decreased.

A 13×20 mm position-sensitive detector[7]) was used which had a resolution of 0.1 mm, ($\equiv < 0.1^{\circ}$) and an energy linearity of better than 1%.

Its 500 μm depletion depth, in conjunction with a 110 μm ΔE detector, enabled up to 70 MeV ^{8}Be events to be detected. Since two ΔE detectors are used in the modified identifier, the area of each detector need only be ∿1/2 as large (5.5×12 mm) for use with the above PSD.

To lessen the effect of kinematic broadening on the ^{8}Be energy resolution, three narrow position gates (X_L, X_C, X_R) were set (see fig. 10b). Each was equivalent to 0.4° and the summed gate (1.2°) had a detection efficiency (ε) of 23-37% for 35-70 MeV ^{8}Be events. In addition, thin targets (∿ 150 μgm/cm^2) were used and rotated to reduce the combined effect of the differential energy loss in the target and the beam spot size.

A ^{8}Be energy spectrum accumulated in two hours from the ^{11}B(α, ^{8}Be)^{7}Li reaction at θ_{lab} = 20° and E_α = 72.5 MeV is shown in fig. 12. This spectrum was obtained by summing the kinematically corrected energy spectra corresponding to the three position gates. Over 25 MeV of excitation in ^{7}Li is observed, and the main transitions to the ground and second excited states are obtained with better energy resolution and lower background than was seen in fig. 6. Also indicated are transitions to the 7.47 MeV; $5/2^-$ and the 0.48 MeV; $1/2^-$ states (the latter only partially resolved). The $5/2^-$ and $1/2^-$ states are expected to be less strongly excited on the basis of calculated α-structure factors[4]). The absolute cross section to the ground state is 16 μb/sr at this energy and angle. The observed energy resolution is 400 keV and the counting rate in each ΔE detector was 25 K cps. At this counting rate the deadtime (measured by a pulser triggered by a monitor counter) is 35%.

Using the modified identifer, data could be collected at twice the rate and with a lower background level than was possible with the simple identifier

(compare figs. 6 and 12). The average background level above the ground state in fig. 12 corresponds to an absolute differential cross section limit of $\sim$ 0.1 μb/sr. Lower cross section limits could be achieved if necessary by reducing the counting rate. (Regarding background from $^{8}Be^{*}$(2.9 MeV) when using a modified identifier, its large breakup Q-value coupled with the restriction on the separation angle of the two α-particles ($\leqslant 6°$) imposed by the divided collimator causes α_1 and α_2 to have sufficiently different energies that the TAC SCA and R SCA requirements eliminate $^{8}Be^{*}$ events from the energy spectra.)

Figure 13 presents a ^{8}Be energy spectrum of the $^{16}O(\alpha,^{8}Be)^{12}C$ reaction at $\theta_{lab} = 23°$. This spectrum was obtained by bombarding a 220 μgm/cm^2 SiO_2 target with 72.5 MeV α-particles and by summing the kinematically corrected energy spectra from the three position gates. Transitions can be clearly seen to the ground and first three excited states and to the 14.08 MeV (4^+) state. The observed energy resolution in fig. 13 is 400 keV and the absolute cross section to the $^{12}C_{gs}$ is 13 μb/sr.

7. Gas Targets

By introducing an additional divided collimator nearer to the target, both the simple and modified ^{8}Be identifiers can be used to study the (α, ^{8}Be) reaction on gas targets. The front collimator defines the extent of the target and removes the possibility of detecting reaction products from the gas cell walls (see fig. 7). To reduce the singles counting rate in the ΔE detectors, a 0.5 mm tantalum partition connects the posts of the two collimators. This partition eliminates particles passing through different sides of the front and back collimators.

An energy spectrum of the (α, ^{8}Be) reaction on a ^{15}N gas target is shown in fig. 14. This spectrum was collected at $\theta_{lab} = 19^{\circ}$ and $E_{\alpha} = 72.5$ MeV with a simple identifier which had twin transmission detectors acting as a large area ΔE detector (of thickness 190 μm). The singles coupling rate was 15 K cps in each of the ΔE detectors. Transitions to several states in ^{11}B can be seen. Those indicated are some transitions expected on the basis of theoretical calculations[4]).

8. Breakup Distribution

By measuring the detection efficiency for monenergetic ^{8}Be events, from the ^{12}C(α,^{8}Be)^{8}Be reaction, with four open circular collimators[12]) of different diameters, one can determine whether the detected α-particles have a radial distribution across the breakup cone consistent with the expected one. Figure 15 presents measured efficiency (ε) points compared with calculated ones[13]), using a 1° position gate. Good agreement is obtained between the experimental and calculated values at the two ^{8}Be energies.

To carry out these measurements, remotely movable collimation was employed with a simple identifier. Any of five different collimators drilled in a single piece of tantalum could be placed in front of the ΔE-E(PSD) telescope. Different collimation, to within 0.1° of the same angle of observation, was made possible by moving the rectangular piece of tantalum in a veritical slide. Changing the collimation rotated a helipot, and the location of the collimators was determined remotely by reading a voltage across the helipot with a digital voltmeter.

The kinematic focussing of the α-particles from the decay of ^{8}Be nuclei causes the α-particles to be confined to a cone. To establish this focussing, transitions to the ground and first excited states of ^{8}Be, from the ^{12}C(α,^{8}Be)^{8}Be reaction at E_{α} = 65 MeV and θ_{lab} = 25°, were studied. Approximately 47-MeV ^{8}Be events arise from these transitions and the calculated apex angle for their breakup cone is 5.1±0.1 . Spectra collected using two different divided collimators of equal open area and with post widths of 5.4° and 3.6°, respectively, are shown in fig. 16. These spectra, accumulated for equal charge, confirm the kinematic focussing of the two α-particles

following ^{8}Be decay. The inserts show the collimator dimensions relative to the size of the ^{8}Be breakup cone. A simple identifier was used with a ΔE counting rate of 20 K cps and with a 2° central position gate.

9. Conclusions

Both the simple and modified ^{8}Be identifiers were developed for the spectroscopic study of the (α,^{8}Be) reaction on solid and gas targets. Using the techniques described above, high detection efficiencies ($\varepsilon \sim 30\%$) were obtained with low background and good energy resolution at high counting rates. Other simple and multi-particle transfer reactions, such as (^{9}Be,^{8}Be), (^{6}Li,^{8}Be), (^{11}B,^{8}Be) and (^{12}C,^{8}Be), should have large enough absolute cross sections on light targets ($d\sigma/d\Omega > 5$ μb/sr) to be easily studied with the simple identifier. Other cases for which the cross section is lower--for example, the (α,^{8}Be) reaction on some s-d shell targets--will require the use of the more sophisticated modified identifier. For either investigation, these techniques greatly simplify the study of reactions involving the detection of ^{8}Be nuclei, opening up the possibility of their more extensive observation in the future.

Acknowledgments

We wish to thank Roy Burton for his help on mechanical design, Don Landis and Ed Lampo for their development work on the electronics and Jack Walton for fabricating the transmission detectors.

Footnotes and References

1) R. E. Brown, J. S. Blair, D. Bodansky, N. Cue, and C. D. Kavaloski, Phys. Rev. 138 (1965) B1394.

J. G. Cramer, K. A. Eberhard, N. R. Fletcher, E. Mathiak, H. H. Rossner, and A. Weidinger, Nucl. Instr. Methods 111 (1973) 425.

K. S. Jayaraman and H. D. Holmgren, Phys. Rev. 172 (1968) 1015.

H. Ho, D. Dehnhard, W. Dünnweber, K. Mudersbach, and J. P. Wurm, Jahresbericht 1972, Max-Planck-Institut Für Kernphysik, Heidelberg, Germany. Also see references in the above.

2) G. J. Wozniak, H. L. Harney, K. H. Wilcox, and J. Cerny, Phys. Rev. Letters 28 (1972) 1278

A. Menchaca-Rocha, Oxford-NP-40-73, Oxford University.

3) G. J. Wozniak, N. A. Jelley, and Joseph Cerny, Phys. Rev. Letters 31 (1973) 607.

4) D. Kurath, Phys. Rev. C7 (1973) 1390.

5) The average value of $\sin 2\gamma$ was calculated with the FORTRAN program EFFICR. In this program the approximation $\beta_1 = \beta_2$ is made, leading to an estimated error in the calculated efficiencies of less than 5.2% for 35-70 MeV ^{8}Be events. This program also calculates the breakup α-particle velocity distribution and is available from the authors on request.

6) Specified counting rates (K CPS) give the number of counts in thousands averaged over one second.

7) Our PSDs were obtained from Edax International, Incorporated.

8) This strong dependence of the PI signal on the fraction of the total energy deposited in the counter telescope is due to an end of the range effect.

9) All excitation energies and spin and parity assignments quoted are from F. Ajzenberg-Selove and T. Lauritsen, Nucl. Phys. A114 (1968) 1 and Nucl. Phys. preprints for A = 6, 7 and 8 (LAP-115, 117).

10) D. Robson, Nucl. Phys. A204 (1973) 523. See Cremer et al., reference 1) for a discussion of a method for detecting $^{8}Be^{*}$ events.

11) G. W. Butler, A. M. Poskanzer, and D. A. Landis, Nucl. Instr. Methods 89 (1970) 189.

12) A divided collimator was not necessary because the $(\alpha, ^{8}Be)$ Q-value is more positive than that of the $(\alpha, ^{7}Li)$ reaction on ^{12}C or ^{13}C. The open circular collimator is also the best to employ since the differential efficiency $(d\varepsilon/dX)$ is more uniform across the 1° position gate.

13) An open collimator has approximately twice the efficiency (ε) of a divided one. However, it has only an ∿20% larger relative efficiency, with a similar dependence of ε_{rel} on E_8 and D.

Figure Captions

Fig. 1. a) Kinematic focussing of the α-particles from the decay of a ^{8}Be nucleus with a kinetic energy (E_8) greater than 35 MeV. Depicted: ^{8}Be velocity vector (v_8); center of mass (c) and laboratory (v_1 and v_2) velocity vectors of the breakup α-particles, and the angle in the center of mass (γ) and the laboratory (β_1) at which α_1 is emitted relative to v_8. b) An illustration of the cone, within which the breakup α-particles are confined. Depicted: distance from target to detector (D), maximum angle in the laboratory (β_{max}) at which a breakup α-particle is emitted relative to v_8, and the radius of the breakup cone (r_m).

Fig. 2. a) Determination of the ^{8}Be event's energy and direction using a PSD. (See discussion in text.) b) A schematic diagram of the simple ^{8}Be identifier showing the divided collimator, transmission detector and PSD.

Fig. 3. a) The dependence of Ω_{eff} on the post width (P) for two collimator diameters ($\mathscr{D}$). E_8 is in MeV and d_m is the calculated diameter of the breakup cone for a 50 MeV ^{8}Be event. b) Calculated ε and ε_{rel} for collimators of different diameters, each having a post width of 0.4 d_m. Other symbols are defined in the text.

Fig. 4. An electronics block diagram for the simple ^{8}Be identifier.

Fig. 5. Position (a) and particle identification (b) spectra obtained with the simple ^{8}Be identifier. (See text.)

Fig. 6. A ^{8}Be energy spectrum of the ^{11}B(α,^{8}Be)^{7}Li reaction taken with the simple identifier.

Fig. 7. A schematic diagram of the modified ^{8}Be identifier, here employed with a gas target.

Fig. 8. An electronics block diagram for the modified ^{8}Be identifier.

Fig. 9. A TAC spectrum, $[\Delta E_L(\text{start}) - \Delta E_R(\text{stop})]$, of events originating from the same beam burst. The ratio of the total background to ^{8}Be events decreases from 120% to 1% as various SCA requirements are introduced.

Fig. 10. Particle identification and position spectra obtained with the modified ^{8}Be identifier.

Fig. 11. a) Calculated TAC spectra, $[\Delta E_L(\text{start}) - \Delta E_R(\text{stop})]$, showing the effect of the divided collimator's shape on the relative velocity distribution. b) A ratio spectrum, $[\Delta E_L/(\Delta E_L + \Delta E_R)]$, collected with the PI and X gates shown in fig. 10. c) Measured TAC spectra routed by the ratio gates shown in part b).

Fig. 12. A ^{8}Be spectrum from the ^{11}B(α,^{8}Be)^{7}Li reaction taken with the modified identifier.

Fig. 13. A ^{8}Be energy spectrum from the ^{16}O(α,^{8}Be)^{12}C reaction taken with the modified identifier.

Fig. 14. A ^{8}Be energy spectrum from the ^{15}N(α,^{8}Be)^{11}B reaction taken with the simple identifier and a gas collimator.

Fig. 15. ^{8}Be detection efficiencies at two ^{8}Be energies for open circular collimators of different radii. The experimental points are normalized to the calculated curves at r = 4 mm; statistical error bars are shown.

Fig. 16. Energy spectra from the ^{12}C(α,^{8}Be)^{8}Be reaction taken with two different divided collimators to illustrate kinematic focussing. Depicted in the respective inserts is the size of the breakup cone relative to that of the divided collimator.

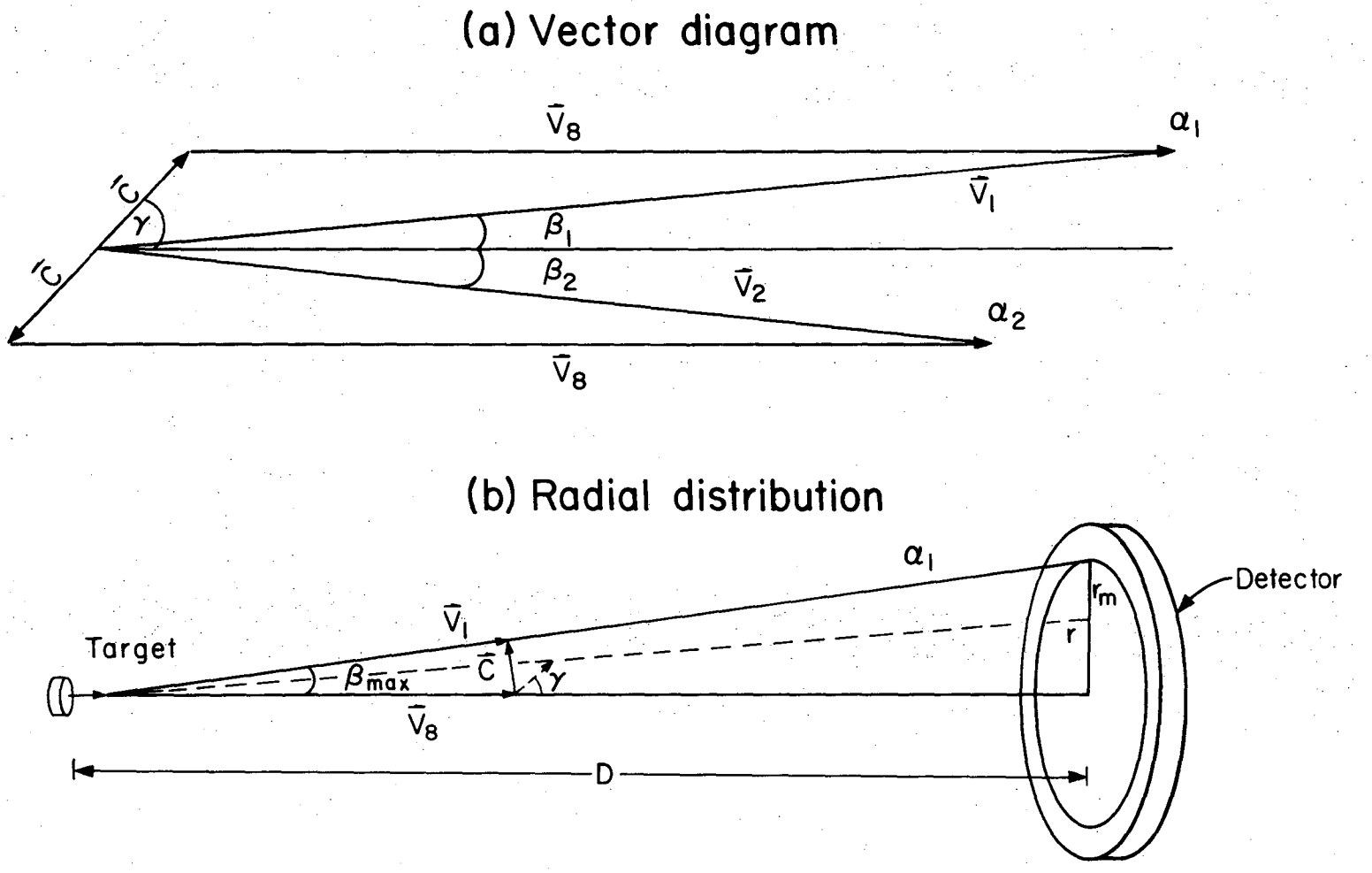

XBL 7311-4447

Fig. 1

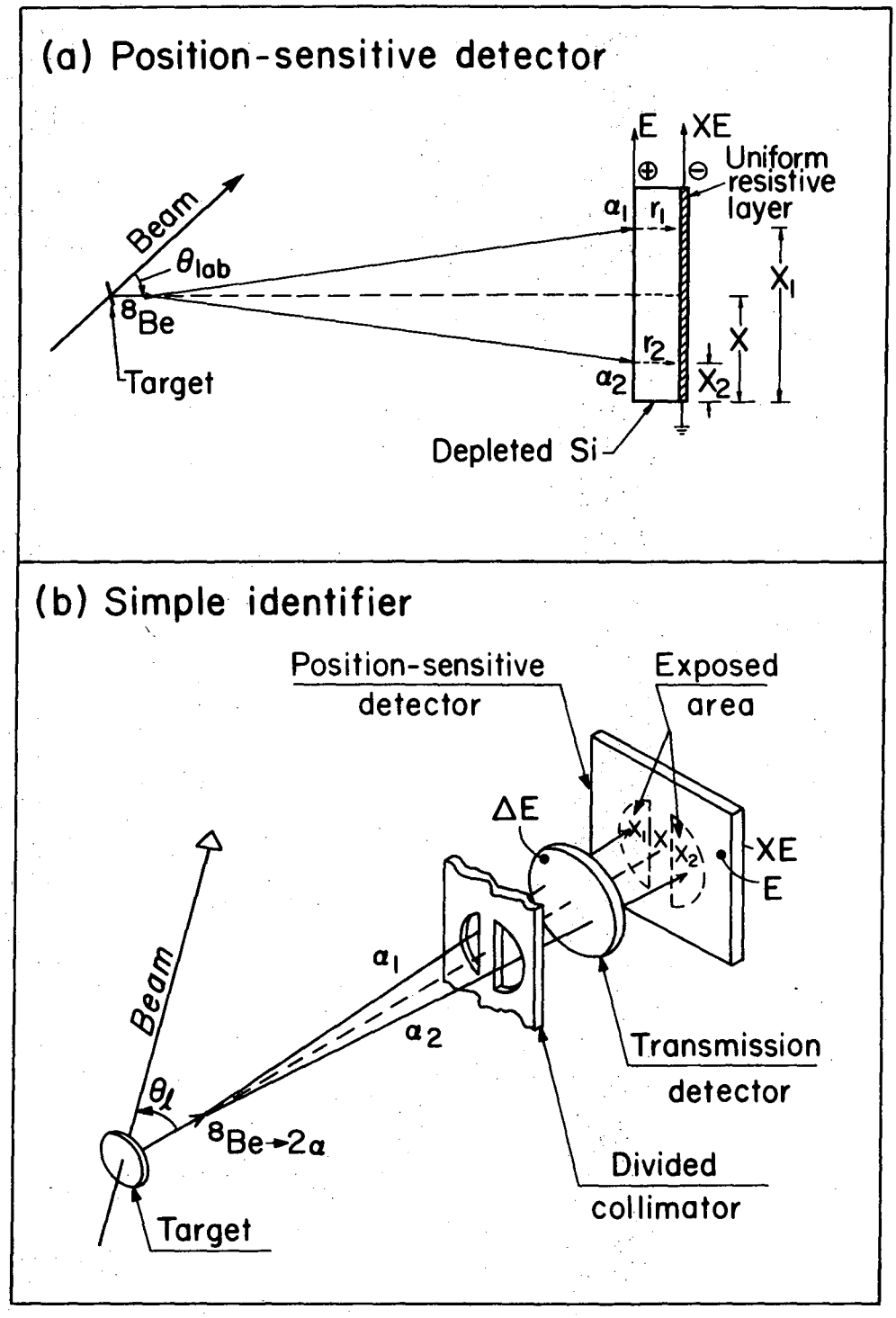

XBL 742-2323

Fig. 2

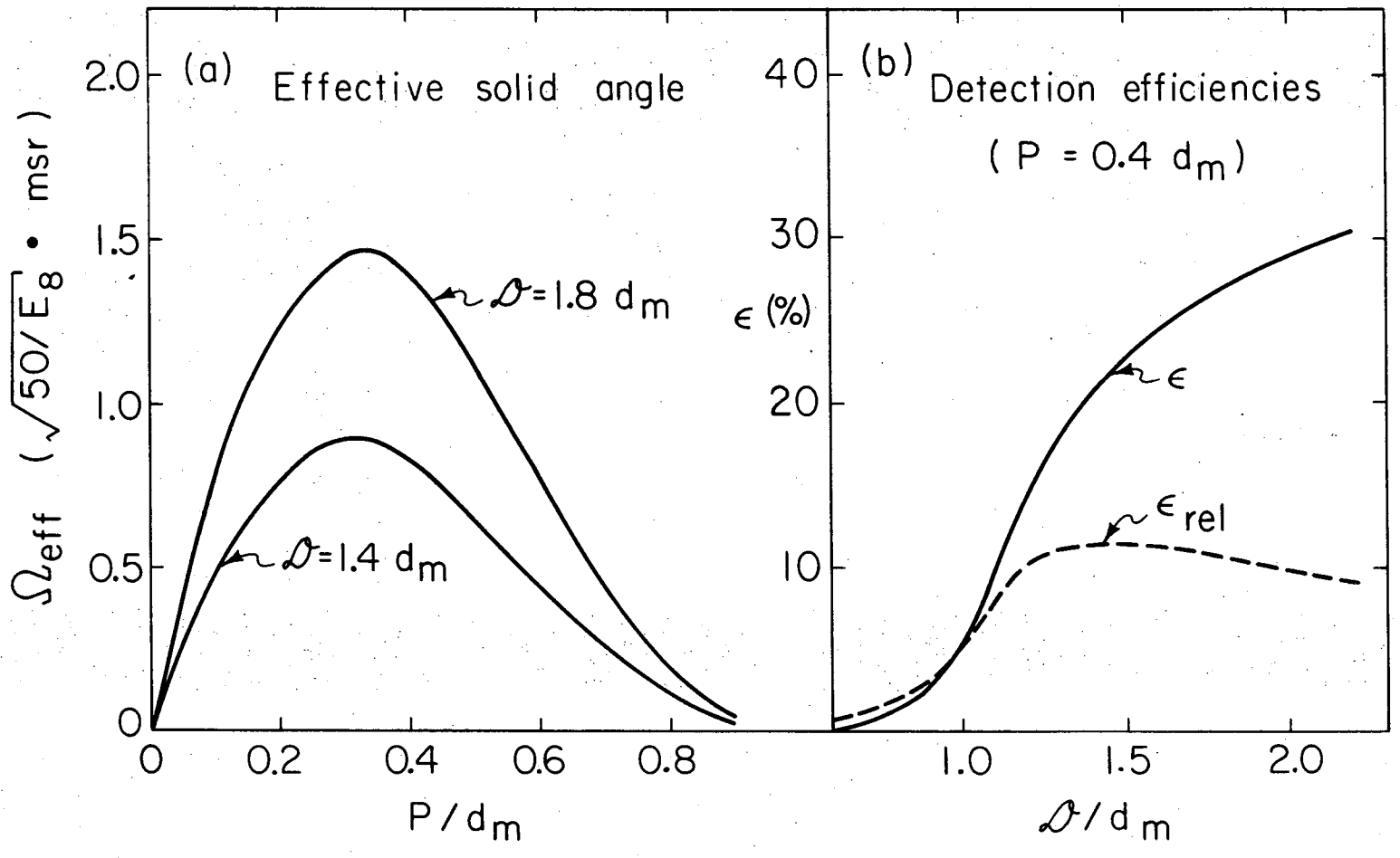

XBL743-2660

Fig. 3

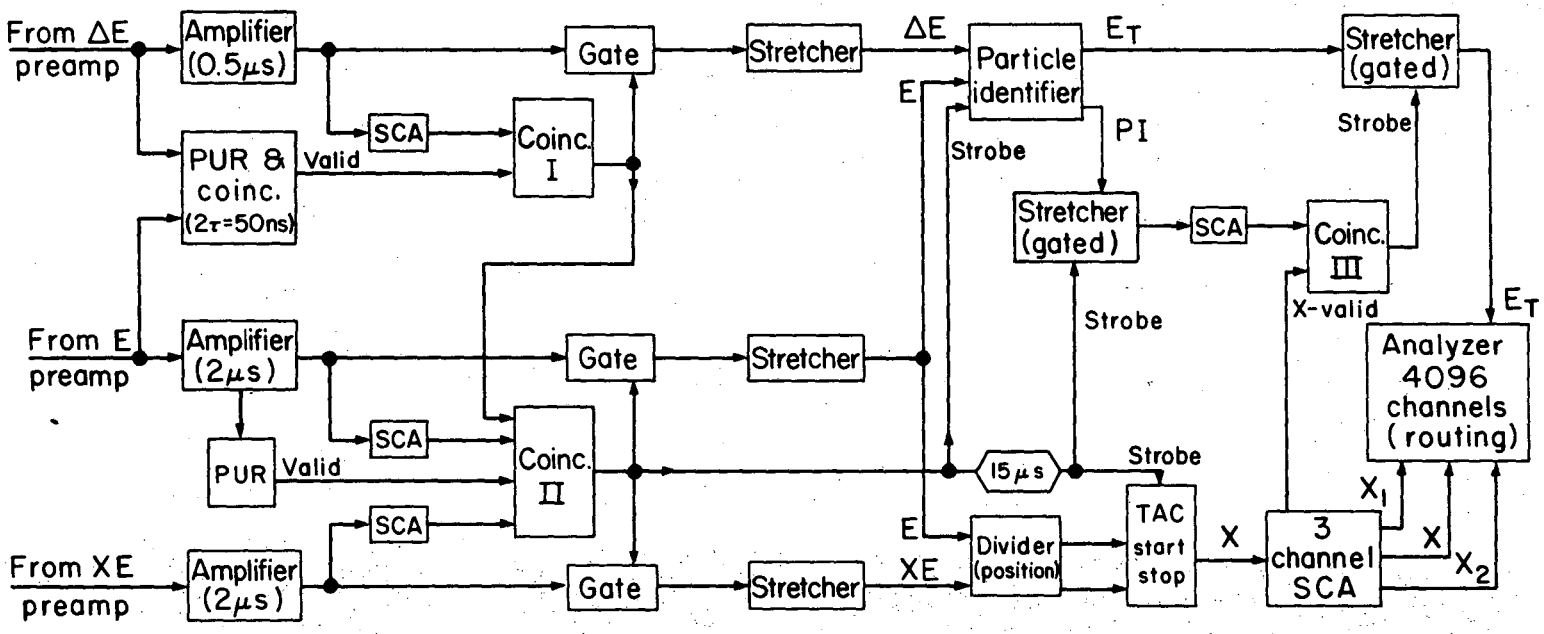

Fig. 4

XBL 742-2321

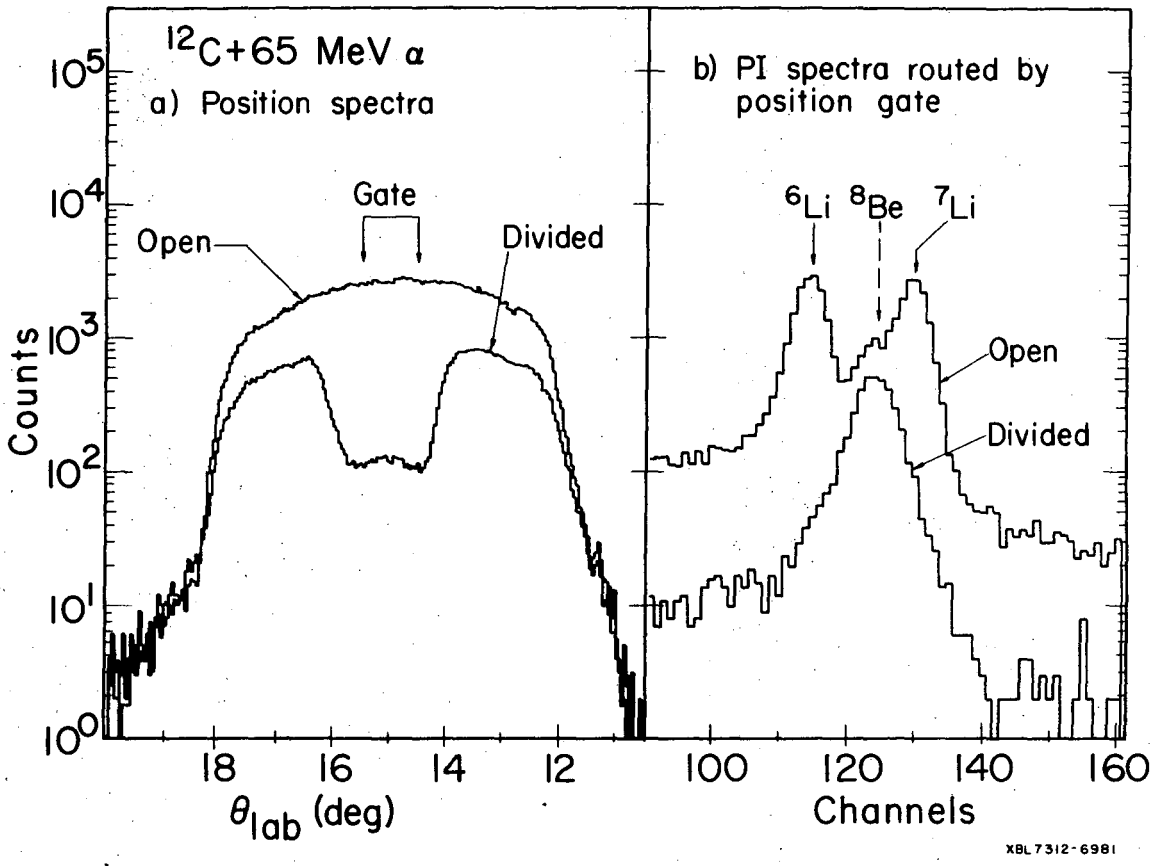
^{12}C+65 MeV α
a) Position spectra
Gate
Open
Divided
Counts
10^5
10^4
10^3
10^2
10^1
10^0
18
16
14
12
θ_{lab} (deg)
b) PI spectra routed by position gate
^{6}Li
^{8}Be
^{7}Li
Open
Divided
100
120
140
160
Channels
XBL7312-6981

Fig. 5

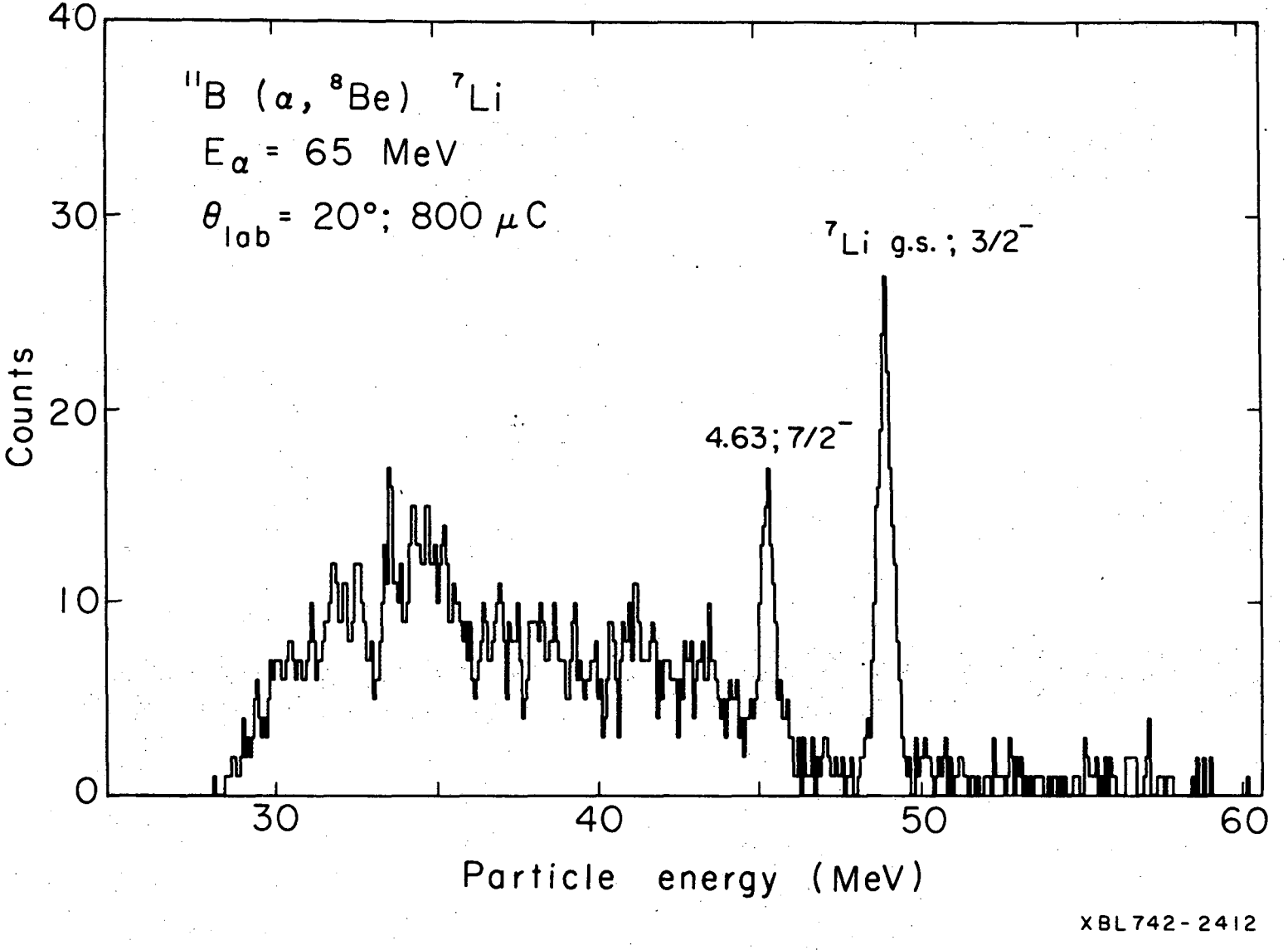

XBL742-2412

Fig. 6

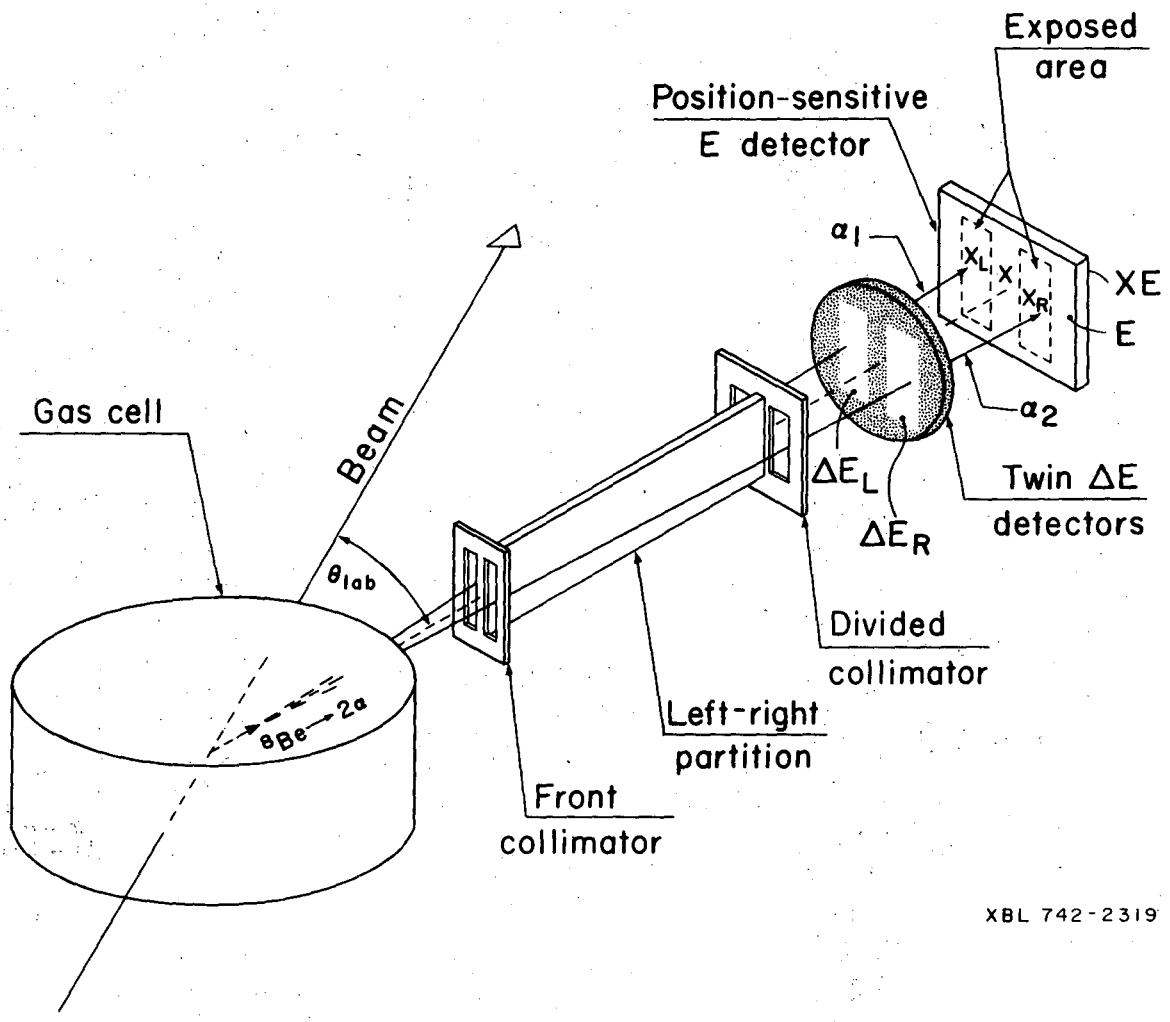
Exposed
area
Position-sensitive
E detector
α_1
X_L
X
X_R
XE
E
α_2
Gas cell
Beam
θ_{lab}
ΔE_L
ΔE_R
Twin ΔE
detectors
Divided
collimator
Left-right
partition
Front
collimator
$^8Be \rightarrow 2\alpha$
XBL 742-2319

Fig. 7

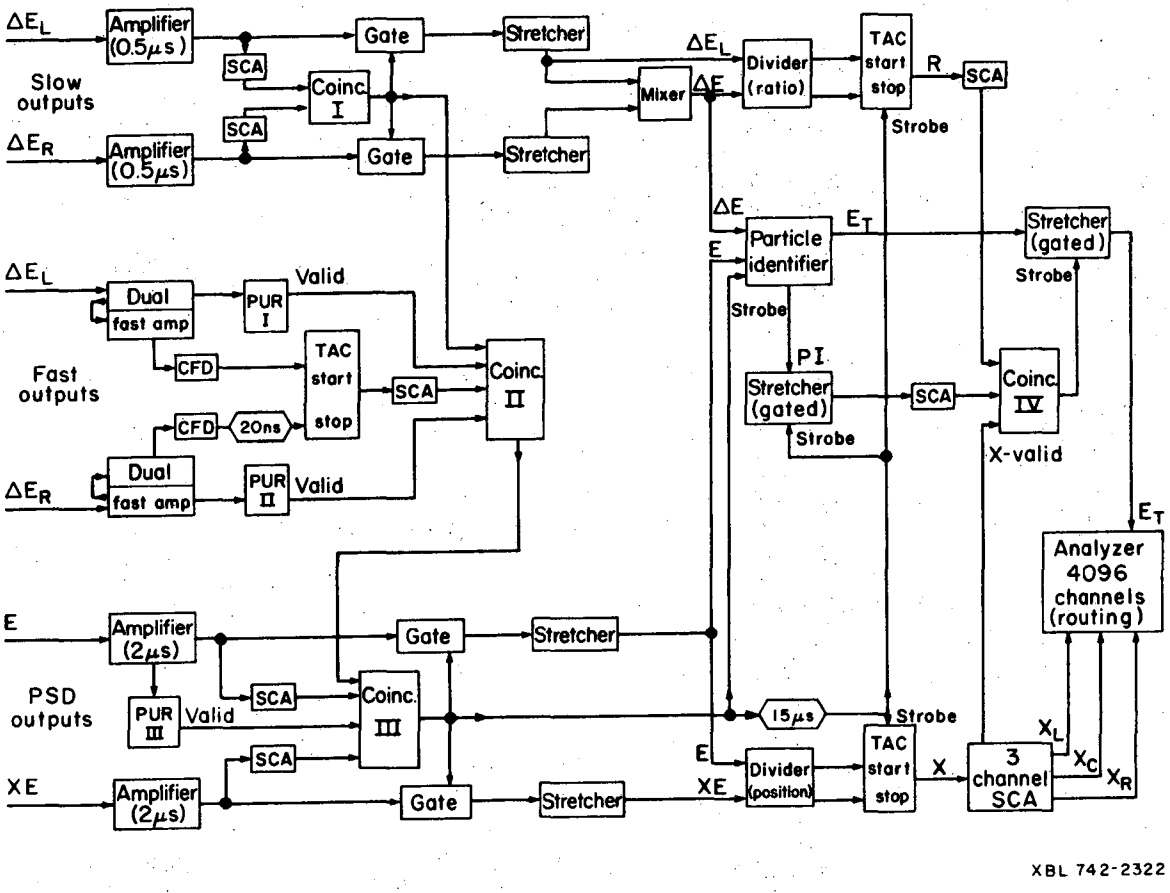
ΔE_L
Amplifier (0.5μs)
SCA
Gate
Stretcher
Slow outputs
Coinc. I
ΔE_R
Amplifier (0.5μs)
SCA
Gate
Stretcher
ΔE_L
Mixer
ΔE
Divider (ratio)
TAC start stop
R
SCA
Strobe
ΔE
Particle identifier
E_T
Stretcher (gated)
Strobe
E
Strobe
PI
ΔE_L
Dual fast amp
PUR I
Valid
Fast outputs
CFD
TAC start stop
SCA
Coinc. II
Stretcher (gated)
SCA
Coinc. IV
Strobe
X-valid
CFD
20ns
ΔE_R
Dual fast amp
PUR II
Valid
E_T
Analyzer 4096 channels (routing)
E
Amplifier (2μs)
Gate
Stretcher
PSD outputs
PUR III
Valid
SCA
Coinc. III
15μs
Strobe
X_L
X_C
X_R
E
XE
Amplifier (2μs)
SCA
Gate
Stretcher
XE
Divider (position)
TAC start stop
X
3 channel SCA
XBL 742-2322

Fig. 8

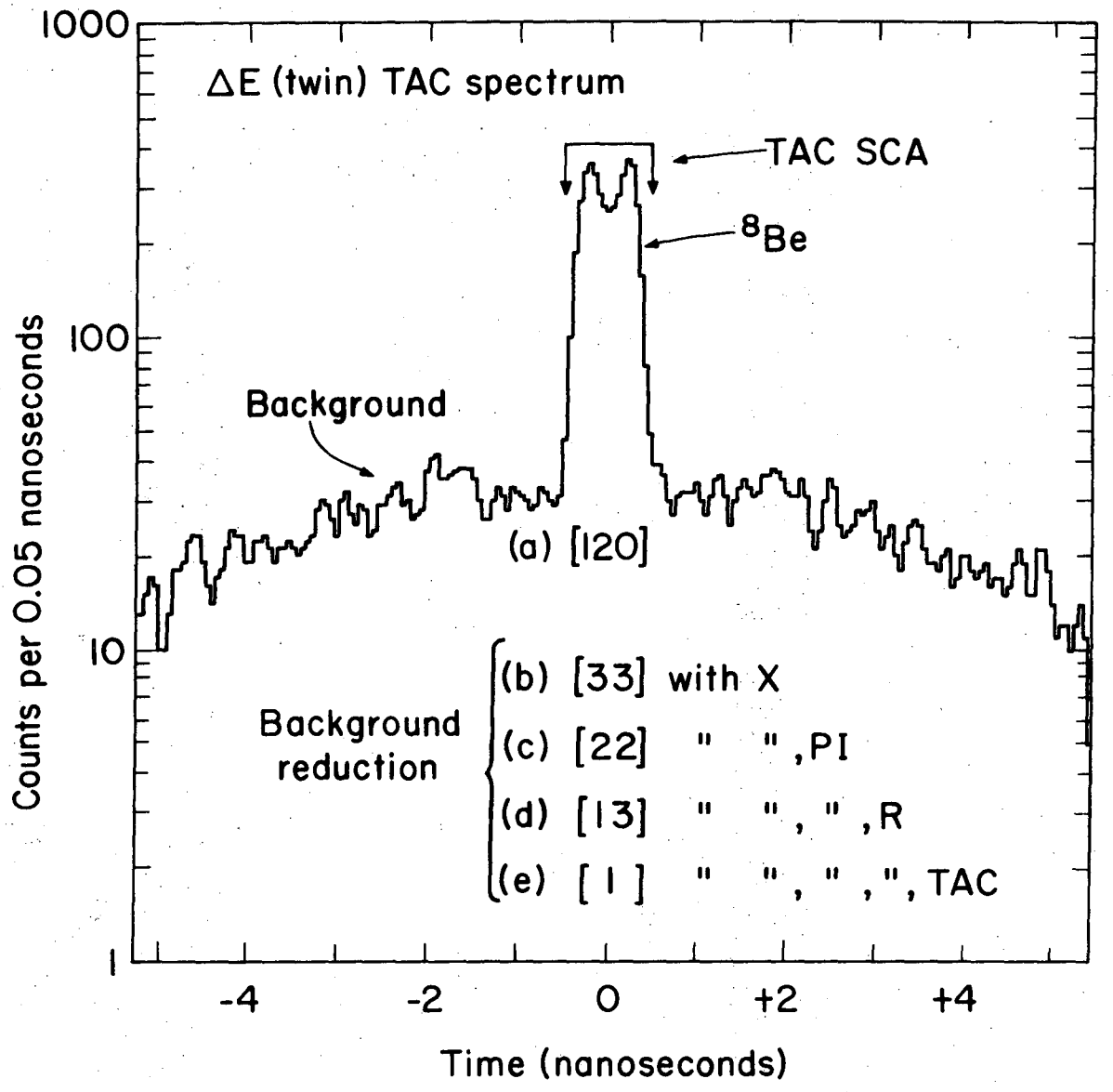

XBL 742-2318

Fig. 9

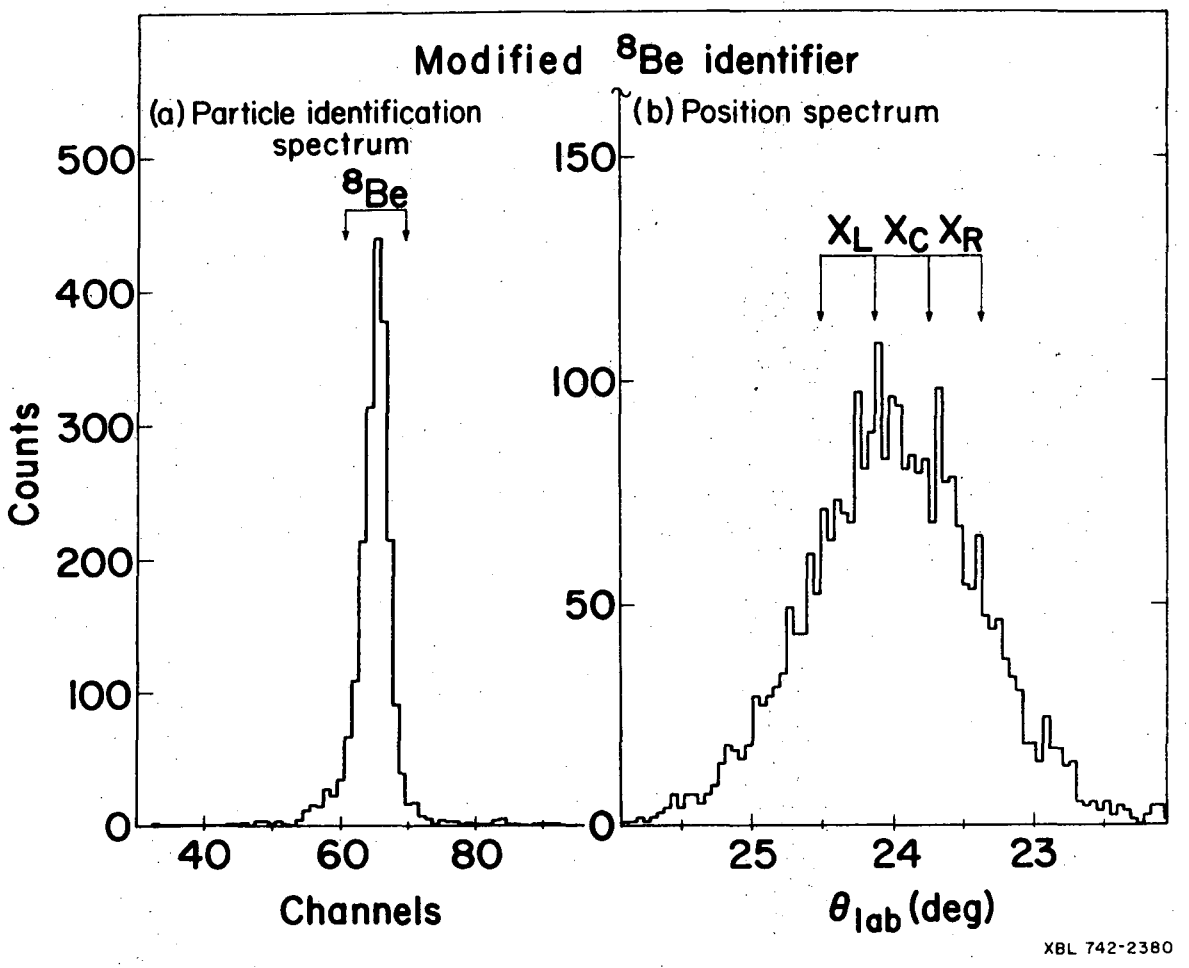
Modified ^{8}Be identifier
(a) Particle identification spectrum
^{8}Be
(b) Position spectrum
X_L X_C X_R
Counts
500
400
300
200
100
0
150
100
50
0
40
60
80
Channels
25
24
23
θ_{lab} (deg)
XBL 742-2380

Fig. 10

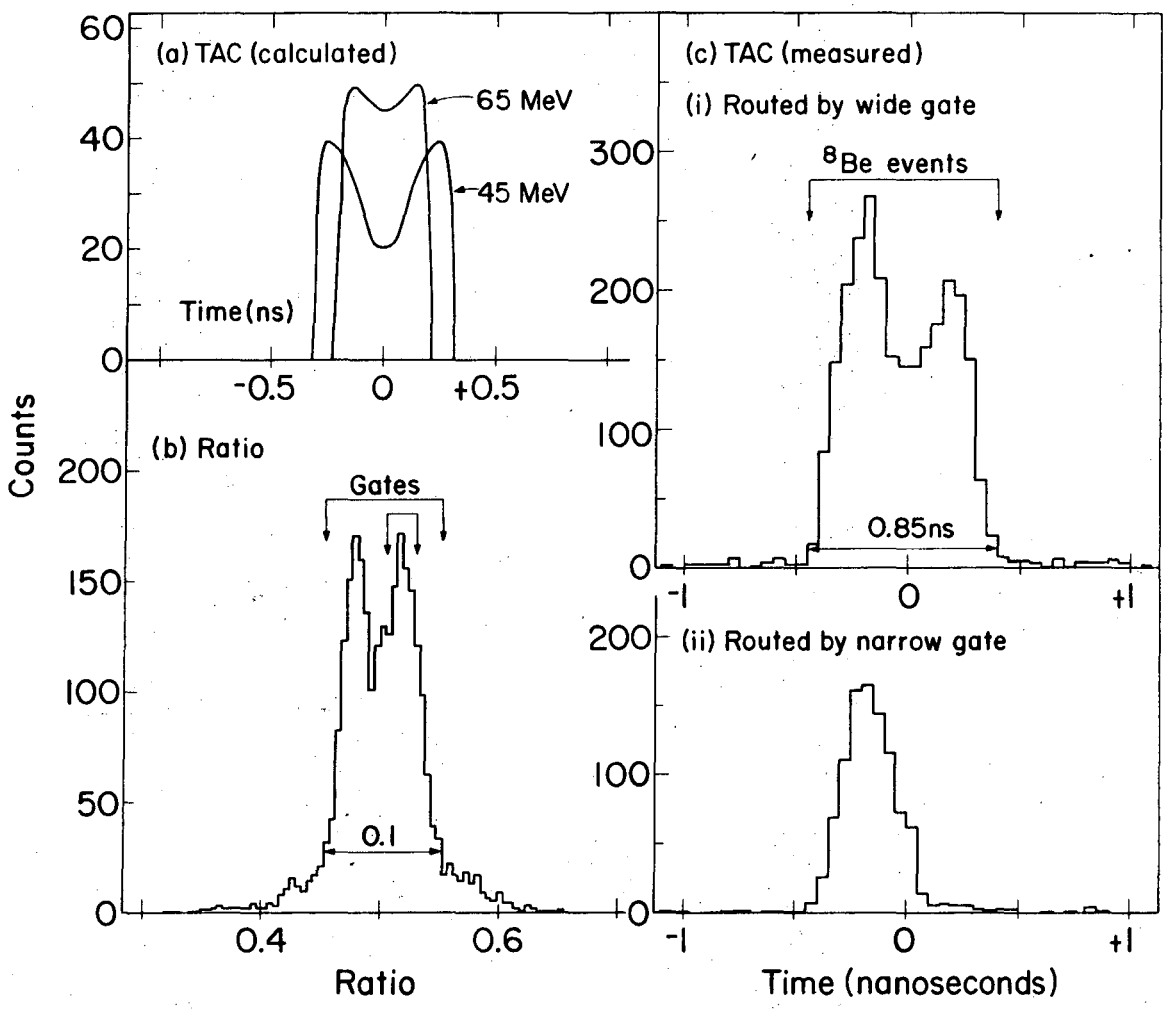
(a) TAC (calculated)
65 MeV
45 MeV
Time(ns)
-0.5
0
+0.5
(b) Ratio
Gates
0.1
Counts
0.4
0.6
Ratio
(c) TAC (measured)
(i) Routed by wide gate
^{8}Be events
0.85ns
(ii) Routed by narrow gate
-1
0
+1
Time (nanoseconds)
XBL 742-2379

Fig. 11

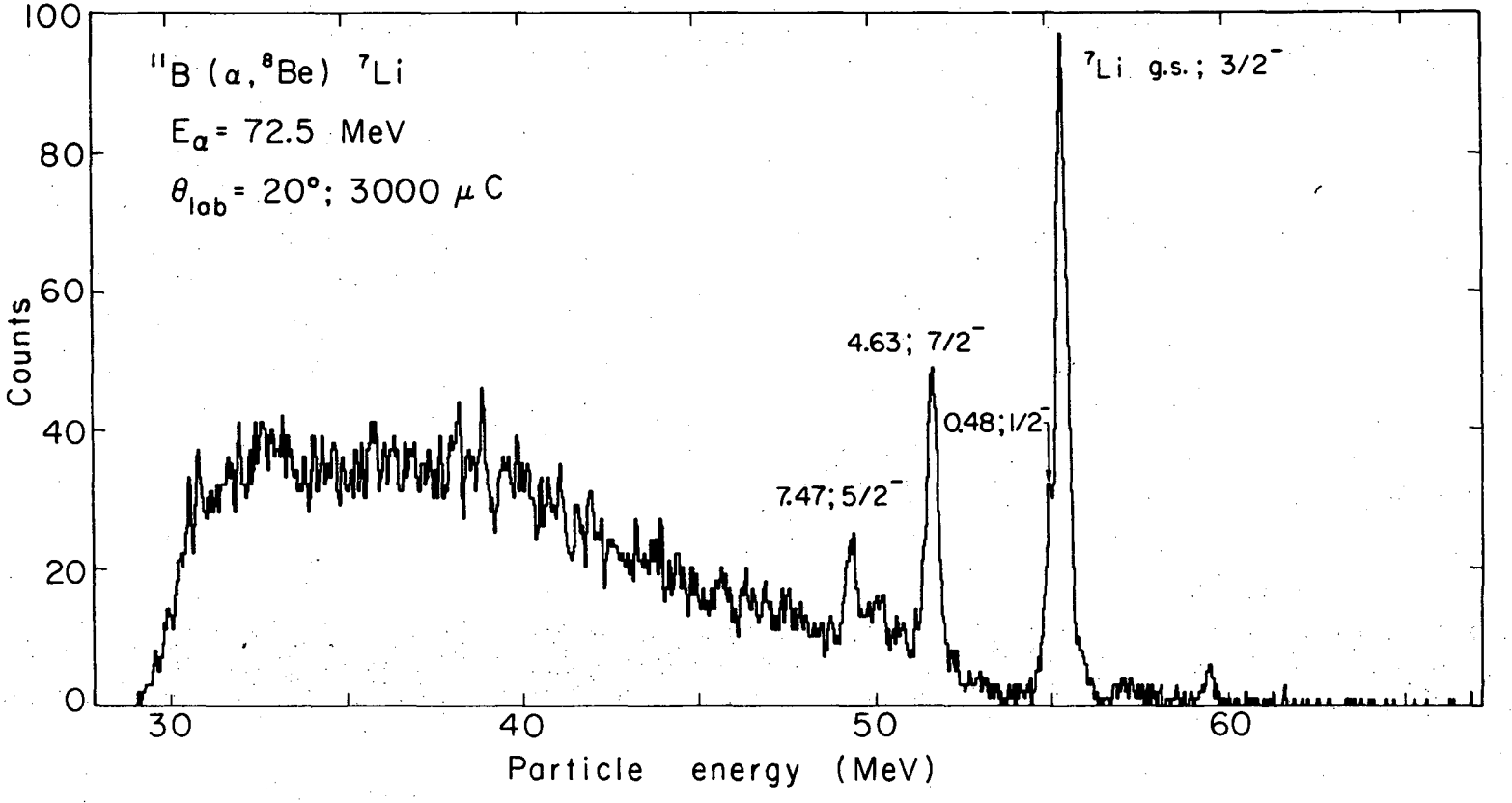

XBL742 - 2411

Fig. 12

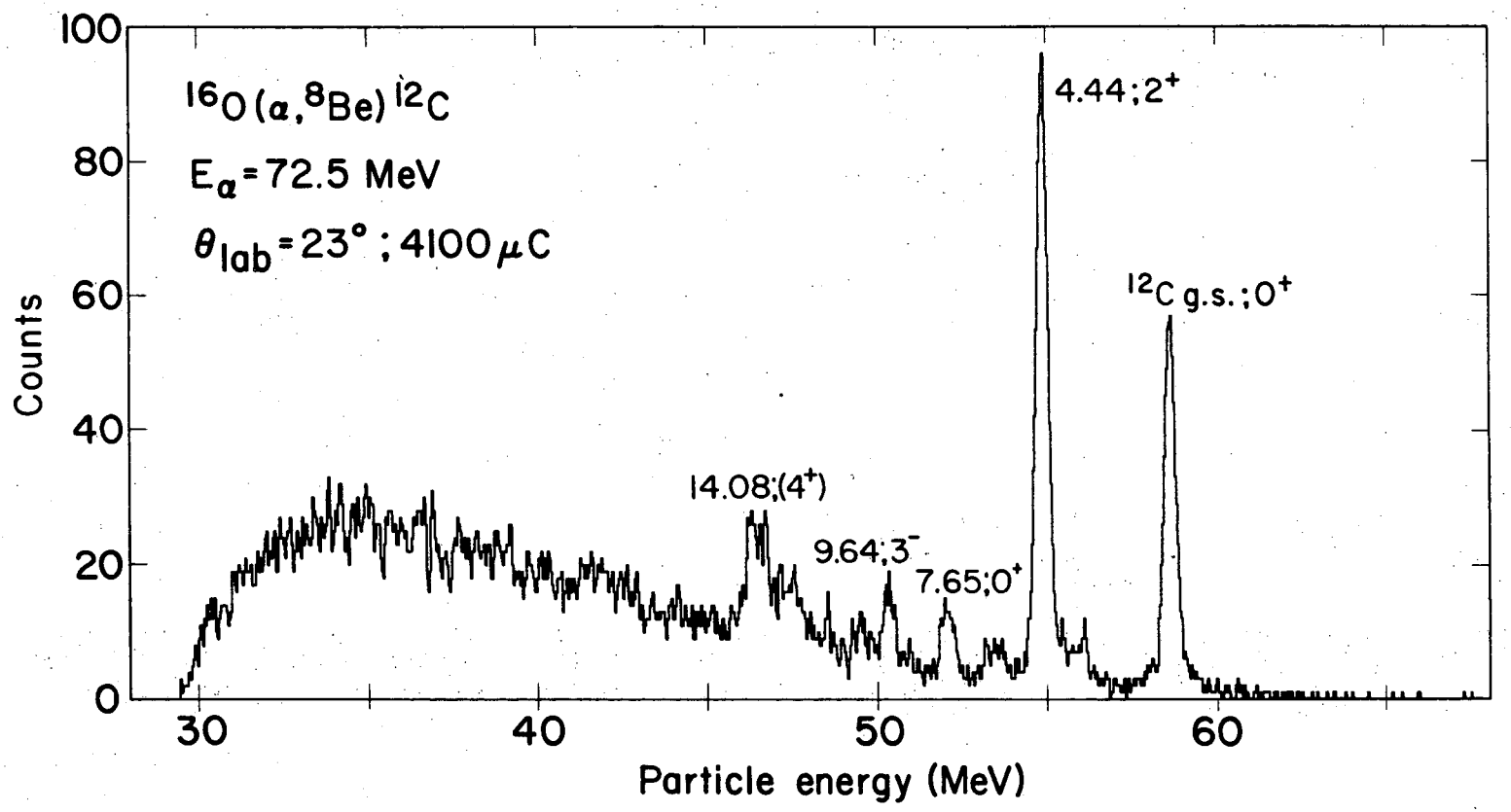

XBL 742-2320

Fig. 13

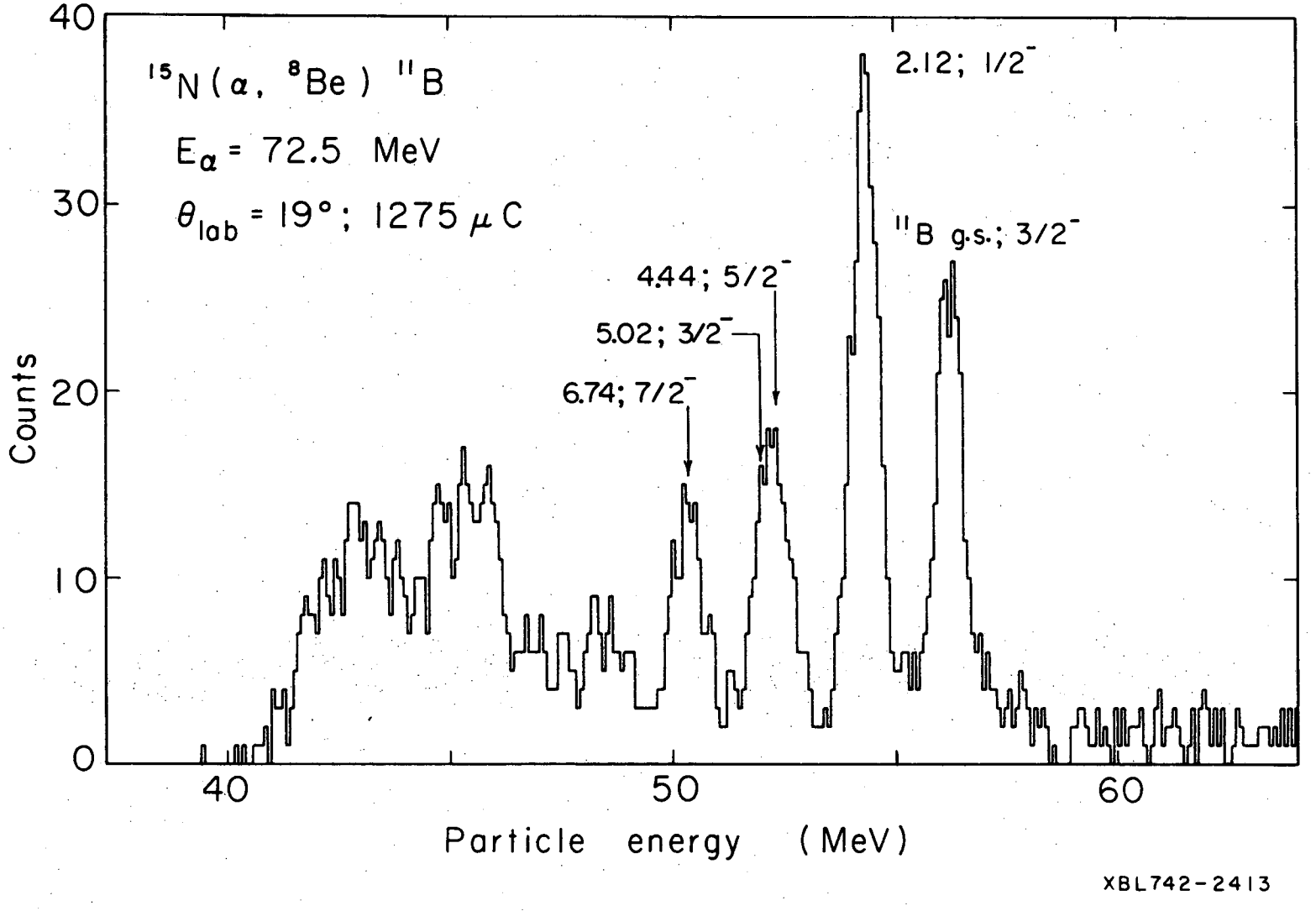
$^{15}N(\alpha, {}^{8}Be)\ ^{11}B$
E_α = 72.5 MeV
θ_{lab} = 19°; 1275 μC
2.12; 1/2⁻
^{11}B g.s.; 3/2⁻
4.44; 5/2⁻
5.02; 3/2⁻
6.74; 7/2⁻
Counts
Particle energy (MeV)
XBL742-2413

Fig. 14

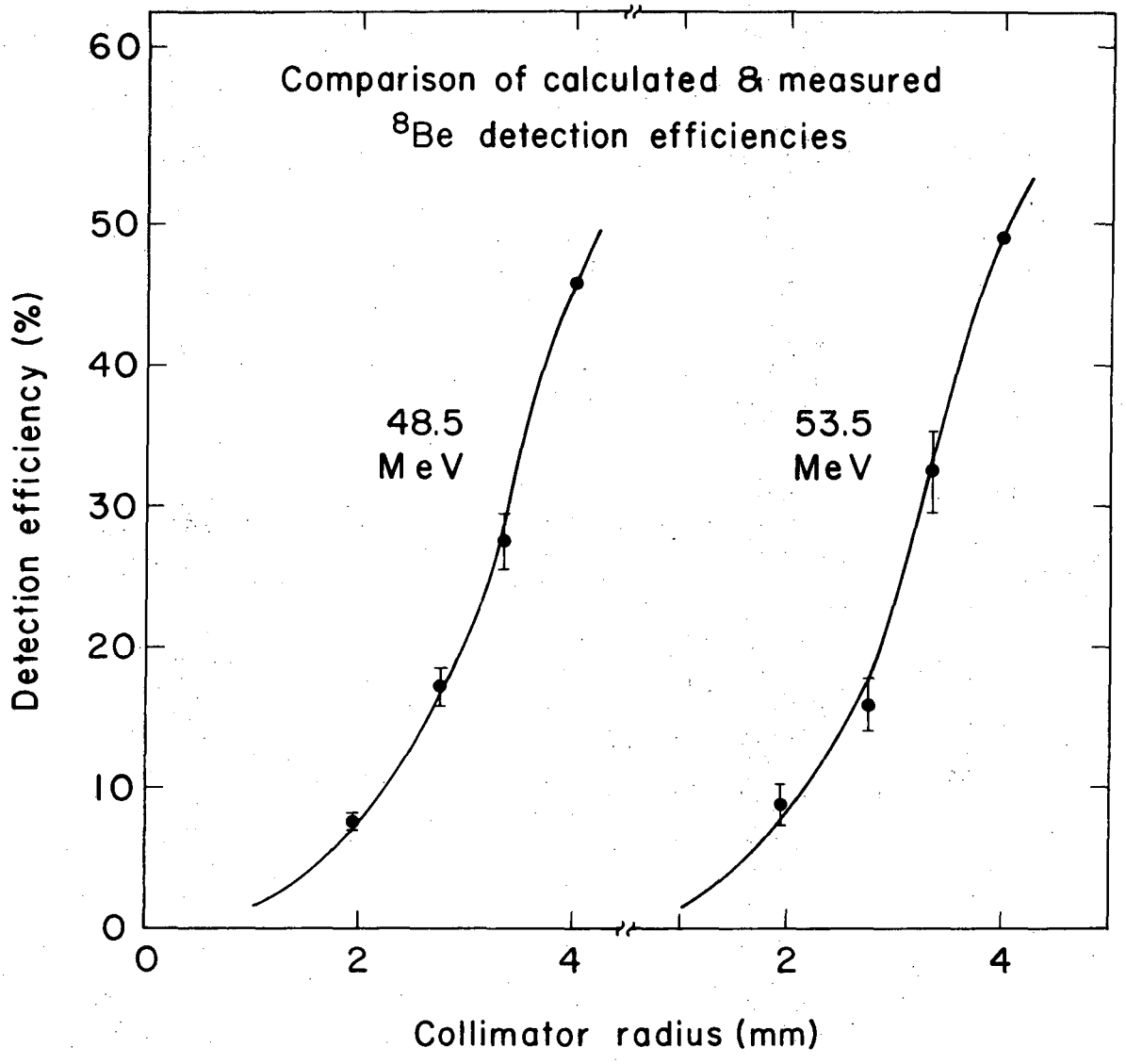

XBL 742-2316

Fig. 15

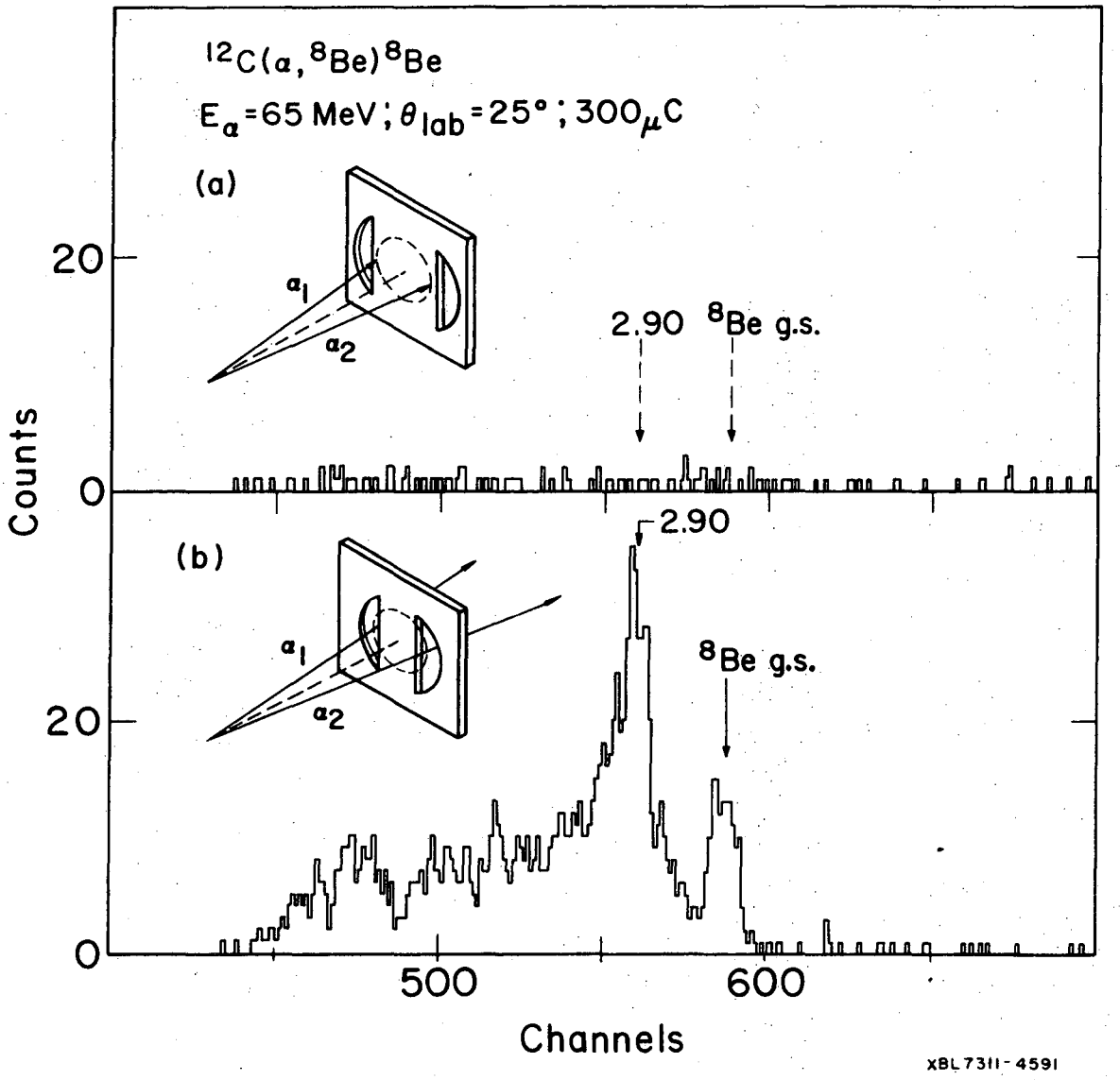
$^{12}C(\alpha, ^8Be)^8Be$
E_α=65 MeV; θ_{lab}=25°; 300μC
(a)
α_1
α_2
2.90
^{8}Be g.s.
(b)
α_1
α_2
2.90
^{8}Be g.s.
Counts
20
0
20
0
500
600
Channels
XBL7311-4591

Fig. 16